Journal of Physics: Conference Series **3027** (2025) 012001 doi:10.1088/1742-6596/3027/1/012001

Finite-size and relativistic effects onto hyperfine interaction of muonic hydrogen

K.L. Franzke[1], W.G. Schmidt[1], U. Gerstmann[1]

[1]Department of Physics, University of Paderborn, Warburger Str. 100, Paderborn, Germany

E-mail: klfra@mail.upb.de

Abstract. Muonic hydrogen is an exotic atom where a muon instead of an electron is bound to a proton. The comparably high mass of the muon ($\approx 207 \cdot m_e$) has two important effects, (i) the reduced mass of the system becomes more important, and (ii) the muon is localized much closer to the nucleus. Thus, muonic hydrogen is not only excellently suitable for evaluating highly precise quantum electrodynamic (QED) calculations, but may also be used for assessing new approaches including finite nuclear size (FNS) effects to evaluate the proton structure and improve calculation schemes for the hyperfine splittings of many-particle systems, as e.g. to be implemented in density functional theory (DFT) software packages. Here, starting from Dirac's equation we calculate the relativistic hyperfine splitting of the ground state and several excited states of muonic hydrogen analytically for different charge and magnetization models. The FNS related hyperfine shifts are compared with the differences between QED calculations and experimental measurements. This comparison also allows to unravel the role of the reduced mass, which is on one hand crucial in case of muonic atoms, but on the other hand is by no means well defined in relativistic quantum mechanics.

1. Introduction

Precise spectroscopy of simple atoms and comparison between theoretical and experimental results is of great importance to evaluate the Standard model, test quantum electrodynamics and obtain high precision values for fundamental physical constants [1, 2, 3, 4, 5]. One of these atoms is muonic hydrogen (μ^1H). It is formed when a muon instead of an electron is bound to a proton. Due to the higher mass of the muon compared to the electron ($m_\mu \approx 207 \cdot m_e$), the muon appears in a region much closer to the nucleus (see also Figure 1) significantly changing the physics of the related muonic atoms and molecules. A well known consequence is e.g. muon catalyzed cold fusion, where thanks to the factor-of-207 smaller atomic radii, deuterium (d, μ^2H) and tritium (t, μ^3H) in a muonic d-t$^+$ molecule can undergo nuclear fusion already at room temperature or even below [6, 7]. In general, the interaction of the muon and the proton is

Journal of Physics: Conference Series **3027** (2025) 012001 doi:10.1088/1742-6596/3027/1/012001

strongly enhanced. As the hyperfine splitting (HFS) reflects the interaction between the magnetic moment of the proton with that of the muon, the HFS of the hydrogen isotopes μ^1H, μ^2H, and μ^3H is therefore especially sensitive to the nuclear structure [8, 2, 9, 10]. Its investigation is, thus, e.g. interesting when it comes to the dermination of the proton charge radius [8, 11, 12, 13]. The experimental value for the proton radius obtained from measurements of the Lamb shift in μ^1H differs from the recent CODATA value, which is known as the proton radius puzzle [13, 14]. An accurate theoretical prediction of the HFS is limited by finite nuclear size (FNS) effects and two-photon exchange (TPE) [15, 9, 16]. One possible solution to the proton radius conundrum could be that the TPE and FNS terms have not been evaluated correctly [13]. Prospectively, their accuracy needs to be elevated to a higher level due to the higher accuracy of upcoming experiments by the CREMA, FAMU and J-PARC collaborations [17, 18, 19, 20, 21]. Thus the investigation of new approaches to include FNS effects appears worthwhile and is the purpose of the present work.

In addition to the growing importance of core-near contributions to the hyperfine splitting, there is a further important characteristic feature of muonic atoms. Due to the higher approximity of muon and proton mass ($m_\mu \approx 0.11 \cdot m_p$), the simple use of the free muon mass m_μ in the calculations is no longer sufficient. In classical, i.e. non-relativistic systems the concept of reduced mass $m_\mu^{\text{red}} = \frac{m_p m_\mu}{m_p + m_\mu}$ is routinely used to solve a two-body problem as an effective one-particle problem. It requires, however, the principle of simultaneity, and thus does not apply to a relativistic two-body system [13, 22, 23]. Nonetheless, the overall substitution $m_\mu \to m_\mu^{\text{red}}$ in Dirac's equation is exact to lowest order in $\frac{m_\mu}{m_p}$ [24], but only for energy levels of unperturbed sytems. In the presence of external vector potentials, the magnetic response of the system is overestimated by a factor $\frac{m_\mu}{m_{\text{red}}}$ yielding (in case of muonic atoms) much too large HFS values.

Here, we analytically calculate the relativistic HFS of the ground state and several excited states of μ^1H and muonic deuterium (μ^2H) for three different nuclear charge and nuclear magnetization models. Beside the standard point-like nucleus with a pure Coulomb potential

$$V(r) = -\frac{Z\alpha\hbar c}{r}$$

and the vector potential

$$\vec{A}(\vec{r}) = \frac{\mu_0}{4\pi}\nabla \times \frac{\vec{\mu}_I}{r} = \frac{\mu_0}{4\pi}\vec{\mu}_I \times \frac{\vec{r}}{r^3},$$

we investigate two finite-size models of the nuclear charge and magnetization density:

(i) The nucleus is considered to be a full sphere with radius R, i.e. with the potentials [25, 26]:

$$V(r) = \begin{cases} -\frac{1}{2}\frac{Z\alpha\hbar c}{R}\left(3 - \frac{r^2}{R^2}\right), & \text{if } r \le R \\ -\frac{Z\alpha\hbar c}{r}, & \text{if } r \ge R \end{cases} \tag{1}$$

Journal of Physics: Conference Series **3027** (2025) 012001 doi:10.1088/1742-6596/3027/1/012001

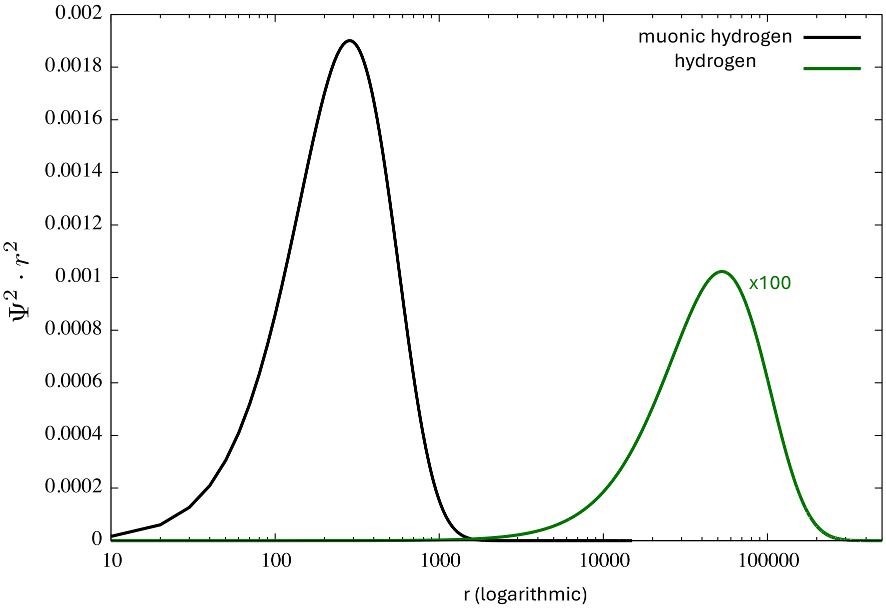

Figure 1. Probability density $|\Psi|^2 r^2$ of the 1s state of muonic and ordinary hydrogen (the latter multiplied by 100). A logarithmic scale on the r axis is used.

and

$$\vec{A}(\vec{r}) = \begin{cases} \dfrac{\mu_0}{4\pi}\dfrac{\vec{\mu}_I \times \vec{r}}{R^3} & \text{, if } r < R \\ \dfrac{\mu_0}{4\pi}\dfrac{\vec{\mu}_I \times \vec{r}}{r^3} & \text{, if } r \geq R \end{cases} \tag{2}$$

(ii) the model of a spherical shell with radius R, i.e. with the potentials [26, 27]:

$$V(r) = \begin{cases} -\dfrac{Z\alpha\hbar c}{R}, & \text{if } r \leq R \\ -\dfrac{Z\alpha\hbar c}{r}, & \text{if } r \geq R \end{cases} \tag{3}$$

and

$$\vec{A}(\vec{r}) = \frac{\mu_0}{4\pi}\frac{\vec{\mu}_I \times \vec{r}}{r^3}\Theta(r-R) = \begin{cases} 0 & \text{, if } r < R \\ \dfrac{\mu_0}{4\pi}\dfrac{\vec{\mu}_I \times \vec{r}}{r^3} & \text{, if } r \geq R \end{cases} . \tag{4}$$

Note that both models are physically reasonable. More realistic distributions of the nuclear magnetization $m(\vec{r})$ are assumed to be somewhere intermediate between the two models [28, 29].

Journal of Physics: Conference Series **3027** (2025) 012001 doi:10.1088/1742-6596/3027/1/012001

2. Hyperfine splitting of muonic hydrogen

2.1. Calculations with QED and from relativistic perturbation theory

Quantum Electrodynamics (QED) allows to calculate the properties of a bound system like muonic or ordinary hydrogen with high precision. The HFS of a one particle system is usually expressed as

$$\Delta^{\mathrm{HFS}} = \Delta_0 \cdot \left(\frac{m_\mu^{\mathrm{red}}}{m_\mu}\right)^3 \cdot \left(1 + \delta^{\mathrm{rel}} + \delta^{\mathrm{QED}} + \delta^{\mathrm{FNS}}\right)$$

where Δ_0 denotes the non-relativistic one-particle Fermi energy which – for muonic atoms – is given by

$$\Delta_0^\mu = \frac{4}{3} m_\mu c^2 (Z\alpha)^3 \alpha g_I \frac{m_\mu}{m_N}.$$

The factor $\left(\frac{m_\mu^{\mathrm{red}}}{m_\mu}\right)^3$ provides the – in case of muonic atoms – extremely important correction for the two-body treatment. The δ terms contain relativistic corrections δ^{rel} and QED corrections δ^{QED} as well as corrections due to the size, structure and polarizability of the finite-size nucleus δ^{FNS} [30]. In some cases it is helpful to calculate specific differences of HFS intervals (e.g. $\Delta_{1s}^{\mathrm{HFS}} - n^3\Delta_{ns}^{\mathrm{HFS}}$) in which nuclear structure corrections cancel to large or even full extend. For other purposes this dependence on nuclear structure properties is welcomed, e.g. when nuclear parameters shall be determined from a comparison between theory and experiment.

The finite nuclear structure contribution can be decomposed into the so-called Zemach term arising from the spatial distributions of the nuclear charge and the nuclear magnetic moment, a two-body recoil term, and an inelastic part. The latter is given by the nuclear polarizability due to nuclear virtual excitations [15, 9, 16, 11, 31] driven by the double exchange of virtual photons between the nucleus and the muon. Thus:

$$\delta^{\mathrm{FNS}} = \delta^{\mathrm{Z}} + \delta^{\mathrm{recoil}} + \delta^{\mathrm{pol}}.$$

The largest contribution is given by the Zemach part [16, 32] which is often estimated by the non-relativistic formula

$$\delta^Z = -2 \cdot Z\alpha\, m_\mu \cdot r_Z$$

where r_Z denotes the Zemach radius, a convolution of the magnetic $m(r)$ and electric charge densities $\rho(r)$ given by [33]

$$r_Z = \int\int \rho(\vec{r}) \cdot |\vec{r} - \vec{r}\,'| \cdot m(\vec{r}\,')\, d^3r d^3r'.$$

Even though the inelastic contributions are non-negligible and required for an accurate description of the absolute HFS values [9], we will focus on the explicitly structure-induced elastic FNS shifts. In Ref. [34], using first-order relativistic perturbation theory these quantities have been successfully calculated analytically without using the non-relativistic Zemach formula for ordinary hydrogen-like atoms. Further details of the

Journal of Physics: Conference Series **3027** (2025) 012001 doi:10.1088/1742-6596/3027/1/012001

method can be found in [34, 35].

In this work we extend the application of this method to muonic hydrogen. Therefore we have to take into account the effect of the reduced mass, which in case of ordinary hydrogen is still negligible [34]. For this purpose we follow the approach of Carroll et al [24] and use the reduced mass m_μ^{red} instead of the free muon mass m_μ in Dirac's equation, but keep the free muon mass in the magnetic moment of the muon by introducing an empirical correction factor of m_μ^{red}/m_μ. We want to emphasize here that this prefactor cannot be analytically derived, but is motivated by analyzing the non-relativistic limit. In a classical, non-relativistic treatment of a quantum mechanical two-body problem with the help of Schrödinger's equation, the reduced mass enters theory naturally by introducing center-of-mass and relative coordinates yielding [36]

$$\Delta_{1s}^{\text{norel}} = \frac{4}{3} m^{\text{red}} c^2 \alpha (Z\alpha)^3 g_I \frac{\left(m^{\text{red}}\right)^2}{m \cdot m_p} = \Delta_0 \cdot \left(\frac{m_\mu^{\text{red}}}{m_\mu}\right)^3 , \tag{5}$$

In relativistic quantum mechanics, however, the concept of the reduced mass is by no means well defined [13, 22, 23] since separation in center-of-mass and relative coordinates is not applicable. A possible empirical approach is suggested by analysing the classical Equation 5. Obviously, the substitution $m \to m^{\text{red}}$ has not to be applied throughout, but is limited to energy and wave function related quantities, suggesting that the mass in the magnetic moment $\frac{e\hbar}{2m} = \mu_B(m)$ has to be left one-particle related as appropriate for this particle property.

Our relativistic approach yields – in case of any spherically symmetric vector potential $\vec{A}(\vec{r})$ – the hyperfine splitting (for further details see [35, 34]):

$$\begin{aligned} \Delta E_{\text{hyperfine}} &= -\, ec\langle\Psi|\vec{\alpha} \cdot \vec{A}(\vec{r})|\Psi\rangle \\ &= -\, \frac{e}{m}\langle\Psi_L|S(r)\vec{A}(\vec{r}) \cdot \vec{p}|\Psi_L\rangle \\ &\quad - \frac{e\hbar}{2m}\langle\Psi_L|S(r)\vec{\sigma} \cdot (\nabla \times \vec{A}(\vec{r}))|\Psi_L\rangle - \frac{e\hbar}{2m}\langle\Psi_L|\vec{\sigma} \cdot (\nabla S(r) \times \vec{A}(\vec{r}))|\Psi_L\rangle \end{aligned} \tag{6}$$

Ψ_L denotes the large component of the bispinor Ψ and $S(r)$ is the so-called relativistic form function. We introduce the reduced mass by substituting $m \to m^{\text{red}}$ in $S(r)$, its derivative and in Dirac's equation for the unperturbed system in order to account for the influence of the reduced mass onto the relativistic wave functions Ψ_L. But we leave the free-particle mass m in the definition of the magnetic moment $\mu_B(m) = \frac{e\hbar}{2m}$, appearing as a prefactor in all three terms of Eq. 6. In case of a two-body system with a point-like nucleus this yields for the HFS of an occupied $1s$ orbital

$$\Delta_{1s} = \frac{1}{\gamma(2\gamma - 1)} \cdot \Delta_0 \left(\frac{m_\mu^{\text{red}}}{m_\mu}\right)^3 , \tag{7}$$

with $\gamma = \sqrt{1 - Z^2\alpha^2}$.
Notably, by substituting $m^{\text{red}} \to m$, Equation 7 becomes again the free-mass formula

Journal of Physics: Conference Series **3027** (2025) 012001 doi:10.1088/1742-6596/3027/1/012001

for the relativistic HFS of a $1s$ state derived by Breit [37].Most importantly, in the non-relativistic limit $\gamma \rightarrow 1$, Eq. 7 yields the classical two-body (reduced-mass including) HFS formula (see Eq. 5) from Schrödinger's theory [36].

3. Results and discussion

In the following we apply the reduced mass corrected, but otherwise analytically exact relativistic calculation of the hyperfine splittings (HFS) [34] to the $1s$ ground state and $2s$, $2p$ excited states of the three muonic hydrogen isotopes μ^1H, μ^2H, and μ^3H. The results are compiled in Table 1. For better comparison the respective data for the electronic sytems are also given.

The values for electronic atoms already have been calculated in our earlier work [34] where the use of the free electron mass m_e has been shown to produce reasonable hyperfine splittings even in case of hydrogen ^{1}H, where the two-body effect manifested by the reduced mass is largest.

3.1. Influence of the reduced mass

In case of muonic hydrogen, due to the 207-times larger mass, the system of muon and nucleus can no longer be treated as a one particle system in a nuclear Coulomb potential. If the free muon mass is used, the calculated hf values are much too large, by about 38% in case of μ^1H, and by about 18% and 12% for muonic deuterium μ^2H and muonic tritium μ^3H, respectively, cf. Tables 1 and A2. Notably, the amount of over-estimization exactly reflects the reciprocal of the reduced mass factor $\left(\frac{m_\mu^{\mathrm{red}}}{m_\mu}\right)^3$ (see also Table A1) which enters theory if the reduced mass is used according to Eq. 6 , i.e. if m_μ^{red} is used in Dirac's equation, but not in the definition of the magnetic moment of the muon [24]. Notably, the agreement is not limited to the case of a point-like nucleus, where the appearance of the mass factor can be motivated analytically according to Eq. 5. It remains in case of finite-size nuclei, modeled via full-sphere or spherical-shell distributions of nuclear charge and magnetization, suggesting that this approach is also exact to first order in $\frac{m_\mu}{m_N}$ in case of finite-size nuclei. Note that the simple and overall substitution $m_\mu \rightarrow m_\mu^{\mathrm{red}}$ in Dirac's equation including the vector potential of the nuclear magnetic moment leads to hf values that are enhanced by 10%. This shows again that the classical concept of reduced mass is rather indeterminate and has to be applied with care in relativistic quantum mechanics [13, 22, 23].

3.2. Influence of finite-size nuclear structure

As has already been observed for electronic hydrogen-like atoms [34], the simple model of a point-like nucleus yields hf values that possess a quite good agreement with experimental data. This agreement is slightly deteriorated when FNS models are used, corresponding with the fact that according to QED other effects such as radiative and recoil corrections need to be taken into account. In other words, the HFS obtained from a Coulomb potential and a point-like magnetic dipole profits in case of light hydrogen-like

Journal of Physics: Conference Series **3027** (2025) 012001 doi:10.1088/1742-6596/3027/1/012001

Table 1. Calculated hyperfine splittings for muonic (in meV) and normal hydrogen (in MHz) for different nuclear charge and magnetization models (for details see text) taking into account the reduced mass [24]. Experimental data taken from [38] ($1s$ state of ^{1}H, ^{2}H, ^{3}H)), [39] (^{1}H $2s$), [40] (^{2}H $2s$), [41] (^{1}H $2p_{1/2}$), [42] (μ^1H $2s$) and [43] (μ^2H $2s$). For the nuclear parameters used to model the finite-size nuclei, see appendix (Table A1).

atom	**state**	**exp**	**model with reduced mass m^{red}**		
		meV		meV	
			point-like	**full sphere**	**spherical shell**
μ^1H	$1s$	—	182.488	181.597	181.413
μ^1H	$2s$	22.809	22.812	22.700	22.677
μ^2H	$1s$	—	49.094	48.457	48.327
μ^2H	$2s$	6.275	6.137	6.057	6.041
μ^3H	$1s$	—	239.943	237.321	236.784
μ^3H	$2s$	—	29.994	29.666	29.599
μ^1H	$2p_{1/2}$	—	7.604	7.604	7.604
μ^1H	$2p_{3/2,\pm 1/2}$	—	1.521	1.521	1.521
μ^1H	$2p_{3/2,\pm 3/2}$	—	4.562	4.562	4.562
		MHz		MHz	
^{1}H	$1s$	1420.406	1418.955	1418.917	1418.909
^{1}H	$2s$	177.557	177.375	177.371	177.370
^{2}H	$1s$	327.834	326.994	326.972	326.968
^{2}H	$2s$	40.925	40.876	40.873	40.872
^{3}H	$1s$	1516.701	1515.160	1515.076	1515.059
^{3}H	$2s$	—	189.401	189.391	189.389
^{1}H	$2p_{1/2}$	59.22	59.125	59.148	59.146
^{1}H	$2p_{3/2,\pm 1/2}$	—	11.824	11.831	11.828
^{1}H	$2p_{3/2,\pm 3/2}$	—	35.472	35.491	35.483

atoms from error cancellation between neglected finite-size and QED-related effects. The main purpose of the present work is, however, not a perfect description of the absolute HFS values, but an as accurate as possible description and evaluation of FNS effects, which are expected to become much more dominant for heavy atoms.

In order to investigate the elastic relativistic FNS effect, we calculate the finite-size induced shifts $\delta_{\text{HF}}^{\text{FN}}$ of the HFS with respect to point-like nuclei (see Table 2) and compare these shifts with the difference between state-of-the-art QED values and experimental data. The elastic FNS shifts due to the spatial distribution of nuclear charge and nuclear magnetic moments are still a challenge in QED [44, 45]. In some cases they have to be neglected, in most cases they can be removed, so that the difference between

Journal of Physics: Conference Series **3027** (2025) 012001 doi:10.1088/1742-6596/3027/1/012001

Table 2. Calculated finite-size induced hf changes $\delta_{\rm hf}^{\rm FS}$ (refering to the point-like case) (using reduced mass $m^{\rm red}$) compared with residual difference between experiment and QED and compared with values calculated in Ref. [24]. For μ^1H, the corrected 6th order QED-values (QED$^*_{(6)}$) are taken from [3, 9] and experimental values from [42]. For μ^2H, estimates for the residual difference (as a measure for the elastic FNS shift) are directly taken from [15]. For the electronic systems (^{1}H, ^{2}H, ^{3}H) the corrected 4th order reference data $E_{\rm hf}^{\rm exp} - E_{\rm hf}^{{\rm QED}^+_{(4)}}$ is taken from [34]. (Residual values for μ^1H($2p$): $\delta_{\rm hf}^{\rm FS} \approx 0.02$ μeV.)

atom	state	$E_{\rm hf}^{\rm exp} - E_{\rm hf}^{{\rm QED}^*_{(6)}}$	Ref. [24]	full sphere this work	spherical shell this work	mixed this work
		μeV	μeV	μeV	μeV	μeV
μ^1H	$1s$	—	—	-891	-1075	-1075
μ^1H	$2s$	-175	-130	-112	-135	-135
μ^2H	$1s$	-984	—	-637	-767	-767
μ^2H	$2s$	-123	—	-80	-96	-96
μ^3H	$1s$	—	—	-2621	-3159	-3159
μ^3H	$2s$	—	—	-328	-395	-395

		$E_{\rm hf}^{\rm exp} - E_{\rm hf}^{{\rm QED}^+_{(4)}}$	full sphere	spherical shell	mixed
		kHz	kHz	kHz	kHz
^{1}H	$1s$	-58	-38	-46	-45
^{1}H	$2s$	-7	-5	-4	-4
^{2}H	$1s$	+2	-23	-26	-26
^{2}H	$2s$	0	-3	-4	-4
^{3}H	$1s$	-85	-84	-101	-101
^{3}H	$2s$	—	-10	-12	-12
^{1}H	$2p_{1/2}$	—	+23	+21	0
^{1}H	$2p_{3/2,\pm1/2}$	—	+7	+4	0
^{1}H	$2p_{3/2,\pm3/2}$	—	+19	+11	0

the resulting advanced (nominally FNS-free) QED data and experiment, $E_{\rm exp} - E_{\rm QED}$, provides a measure for the elastic FNS shift. Whereas for electronic atoms 4th order QED calculations accomplished by nuclear polarization and recoil effects suffice ($E_{\rm hf}^{{\rm QED}^+_{(4)}}$, see also Ref. [34] and [46, 47, 48, 49]), in case of muonic atoms further higher order terms are required.

The $E_{\rm hf}^{{\rm QED}_{(4)}}$ values have to be corrected with various contributions from relativistic, anomalous magnetic moment, vacuum polarization and inelastic FNS corrections of up

Journal of Physics: Conference Series **3027** (2025) 012001 doi:10.1088/1742-6596/3027/1/012001

to 6th order leading to $E_{\rm hf}^{\rm QED^*_{(6)}}$. For muonic systems the remaining data $E_{\rm exp} - E_{\rm QED}$ are in the < 1 meV regime. The corresponding data are available for the $1s$ and $2s$ state of muonic deuterium μ^2H and the $2s$ excited state of μ^1H, exclusively, whereupon the latter provides an exceptional case, which has been already investigated quantitatively by a numerical perturbative approach. For both models, full sphere as well as spherical shell, with our fully relativistic analytical approach we obtain a reasonably good agreement with the available reference data. The spherical shell model yields always (for all investigated muonic states, and also for the electronic ones) 20% larger FNS induced HFS shifts, which are in better agreement with experimental data. Notably, in case of μ^1H ($2s$) they coincides with the – exclusively for this case available – purely theoretically determined value reported by Carroll et al. [24]. In connection with a calculation of the Lamb-Shift between the quasi-degenerate $2s$ and $2p_{1/2}$ levels, the latter authors used a numerical solution of Dirac's equation with an exponential FNS potential and evaluate the hyperfine splitting using a nonrelativistic perturbative formula [50] for the $2s$ HFS.

For the $2p$ states it has been reported, that the use of finite-size potentials has no influence in the limits of the calculations. Our analytical calculations confirm this observation (see also Table 1); residual differences are found around 0.02 μeV.

Interestingly, the overall good agreement with experimental reference data is not limited to the nuclear model of a spherical shell, where both nuclear charge as well as nuclear magnetic moment are distributed on the surface of a spherical shell. Exactly the same data are obtained for a mixed model, where finite-size effects are only taken into account via the vector potential of the nuclear magnetic moment Eq. 4 (see also Table A2).

Already the combination with a point charge (Coulomb potential) is perfectly reproducing the results of the 'full' model.

This fact allows for the promising possibility of obtaining accurate relativistic hyperfine splittings including FNS-effects already based on wave functions from the standard treatment, i.e. using Coulomb potentials, without the need for an explicit solution of Dirac's equation within the nuclear core region.

4. Summary

In this work we have investigated the influence of the proton structure onto the hyperfine splitting of muonic hydrogen. For this purpose a recently presented fully relativistic analytical treatment [34] based on the analytical solution of Dirac's equation for finite-size nuclear potentials has been accomplished by an empirical correction containing the reduced mass [24]. This correction is required due to the higher approximity of muon and proton mass, so that muonic hydrogen can no longer be treated as a particle in an external nuclear potential. Although the classical concept of the reduced mass is not well-defined in relativistic quantum mechanics, we confirm that it can be used to calculate accurate hyperfine splttings if it is applied with care, i.e. if the reduced mass is used in the mass term $m_\mu c^2$ of Dirac's equation, but not in the definition of the magnetic moment of the muon. Using the $1s$ ground state and $2s$, $2p$ excited states of the three muonic hydrogen isotopes μ^1H, μ^2H, and μ^3H of myonic hydrogen as prototype examples, we show that this treatment removes a spurious factor $\left(\frac{m_\mu}{m_\mu^{\rm red}}\right)^3$ and adjusts the

calculated hyperfine splittings to the experimental data, also in case of finite-size nuclei. The nucleus is described as point-like as well as by homogenously charged and magnetized full spheres or spherical shells. Thereby, we do not restrict our study to models with equal treatment of charge and magnetic moment, but also investigate a mixed model, where a spherical-shell distributed nuclear magnetic moment is assumed while retaining a Coulomb potential. Interestingly this mixed model reproduces exactly the hyperfine splitting of the full model, but does not require explicit solution of Dirac's equations within the nuclear core region. It is thus easy to implement in density functional (DFT) packages and should be able to lift the calculation of hyperfine splitting of many-body systems onto the next level of accuracy.

5. Acknowledgments
The authors thank H.-J. Wagner (Paderborn) for helpful discussions. They are also grateful to the Paderborn Center for Parallel Computing (PC^2) for the provided computational resources, as well as funding by the Deutsche Forschungsgemeinschaft (DFG) from TRR 142/3-2024, Project No. 231447078.

References
[1] Mohr P J, Taylor B N and Newell D 2000 *Reviews of Modern Physics* **72** 351
[2] Martynenko A and Faustov R 2004 *Journal of Experimental and Theoretical Physics* **98** 39–52
[3] Martynenko A 2005 *Physical Review A* **71** 022506
[4] Martynenko A 2008 *Physics of Atomic Nuclei* **71** 125–135
[5] Karshenboim S G 2005 *Physics Reports* **422** 1–63
[6] Balin D, Ganzha V, Kozlov S, Maev E, Petrov G, Soroka M, Schapkin G, Semenchuk G, Trofimov V, Vasiliev A, Vorobyov A, Voropaev N, Petitjean C, Gartner B, Lauss B, Marton J, Zmeskal J, Case T, Crowe K, Kammel P, Hartmann F and Faifman M 2011 *Physics of Particles and Nuclei* **42** 185–214
[7] Berlinguette C, Chiang Y M, Munday J, Schenkel T, Fork D, Koningstein R and Trevithick M 2019 *Nature* **570** 45–51
[8] Karshenboim S G, Korzinin E Y and Ivanov V G 2008 *JETP Letters* **88** 641–646
[9] Kalinowski M, Pachucki K and Yerokhin V A 2018 *Physical Review A* **98** 062513
[10] Pachucki K 1996 *Physical Review A* **53** 2092
[11] Antognini A, Hagelstein F and Pascalutsa V 2022 *Annual Review of Nuclear and Particle Science* **72** 389–418
[12] Pohl R, Antognini A, Nez F, Amaro F D, Biraben F, Cardoso J M, Covita D S, Dax A, Dhawan S, Fernandes L M *et al.* 2010 *Nature* **466** 213–216
[13] Pohl R, Gilman R, Miller G A and Pachucki K 2013 *Annual Review of Nuclear and Particle Science* **63** 175–204
[14] Pohl R and collaboration C 2014 *Hyperfine Interactions* **227** 23–28
[15] Ji C, Zhang X and Platter L 2024 *Physical Review Letters* **133** 042502
[16] Hagelstein F, Lensky V and Pascalutsa V 2023 *The European Physical Journal C* **83** 762
[17] Pohl R 2016 *Journal of the Physical Society of Japan* **85** 091003
[18] Dupays A, Beswick A, Lepetit B, Rizzo C and Bakalov D 2003 *Physical Review A* **68** 052503
[19] Adamczak A, Baccolo G, Bakalov D, Baldazzi G, Bertoni R, Bonesini M, Bonvicini V, Campana R, Carbone R, Cervi T *et al.* 2016 *Journal of Instrumentation* **11** P05007
[20] Ma Y, Ishida K, Iwasaki M, Matsuzaki Y, Oishi Y, Okada S, Sato M, Midorikawa K, Saito N, Wada S *et al.* 2016 *International Journal of Modern Physics: Conference Series* vol 40 (World Scientific) p 1660046
[21] Tomalak O 2018 *The European Physical Journal A* **54** 3
[22] Borie E and Rinker G 1982 *Reviews of Modern Physics* **54** 67

Journal of Physics: Conference Series **3027** (2025) 012001 doi:10.1088/1742-6596/3027/1/012001

[23] Ni G J, Xu J J and Lou S Y 2011 *Chinese Physics B* **20** 020302
[24] Carroll J, Thomas A, Rafelski J and Miller G 2011 *Physical Review A* **84** 012506
[25] Xie HH Li J, Jiao L and Ho Y 2023 *Physical Review A* **107** 042807
[26] Moore E and Moss R 1975 *Molecular Physics* **30** 1315
[27] Battocletti M and Ebert H 2001 *Physical Review B* **64** 094417
[28] Schneider S M, Schaffner J, Greiner W and Soff G 1993 *Journal of Physics B: Atomic, Molecular and Optical Physics* **26** L581–L584
[29] Shabaev V M 1994 *Journal of Physics B* **27** 5825–5832
[30] Eides M I, Grotch H and Shelyuto V A 2001 *Physics Reports* **342** 63–261
[31] Carlson C, Nazaryan V and Griffioen K 2008 *Physical Review A* **78** 022517
[32] Zemach A C 1956 *Physical Review* **104** 1771–1781
[33] Krauth J J, Diepold M, Franke B, Antognini A, Kottmann F and Pohl R 2016 *Annals of Physics* **366** 168–196
[34] Franzke K L and Gerstmann U 2024 *Foundations* **4** 513–536
[35] Franzke K L, Schmidt W G and Gerstmann U 2024 *Journal of Physics: Conference Series* **2701** 012094
[36] Borie E 1976 *Zeitschrift für Physik A* **278** 127–131
[37] Breit G 1930 *Physical Review* **35** 1447
[38] Anderson L W, Pipkin F M and Baird J C 1960 *Physical Review* **120** 1279
[39] Matveev A, Alnis J, Parthey C, Kolachevsky N and Hänsch T W 2009 *CLEO/Europe-EQEC 2009-European Conference on Lasers and Electro-Optics and the European Quantum Electronics Conference* (IEEE) pp 1–1
[40] Kolachevsky N, Fendel P, Karshenboim S G and Hänsch T W 2004 *Physical Review A* **70** 062503
[41] Lundeen S, Jessop P and Pipkin F 1975 *Physical Review Letters* **34** 377–380
[42] Antognini A, Nez F, Schuhmann K, Amaro F D, Biraben F, Cardoso J M, Covita D S, Dax A, Dhawan S, Diepold M *et al.* 2013 *Science* **339** 417–420
[43] Pohl R, Nez F, Fernandes L M, Amaro F D, Biraben F, Cardoso J M, Covita D S, Dax A, Dhawan S, Diepold M *et al.* 2016 *Science* **353** 669–673
[44] Jentschura U D and Yerokhin V A 2006 *Physical Review A* **73** 062503
[45] Bullis R, Rasor C, Tavis W, Johnson S, Weiss M and Yost D 2023 *Physical Review Letters* **130** 203001
[46] Khriplovich I, Milstein A and Petrosyan S 1996 *Physics Letter B* **366** 13–17
[47] Patkóš V, Yerokhin V A and Pachucki K 2023 *Physical Review A* **107** 052802
[48] Pachucki K 2022 *Physical Review A* **106** 022802
[49] Pachucki K and Yerokhin V 2023 *Physical Review Letters* **130** 053002
[50] Weissbluth M 2012 *Atoms and Molecules* (Elsevier)
[51] Mohr P, Newell D, Taylor B and Tiesinga E 2024 *arXiv preprint arXiv:2409.03787*

Journal of Physics: Conference Series **3027** (2025) 012001 doi:10.1088/1742-6596/3027/1/012001

Appendix A. Nuclear parameters and free-mass data

Table A1. Parameters used in the calculations: nuclear g-factor g_I, core radius R and mass m_N together with the reduced mass for electronic ($m_e = 9.1093837139 \cdot 10^{-31}$ kg) and muonic ($m_\mu = 1.883531627 \cdot 10^{-28}$ kg) systems. Nuclear charge radii taken from recent CODATA [51].

nucleus	g_I	R [fm]	m_N [10^{-27} kg]	$\left(\frac{m_e^{\text{red}}}{m_e}\right)^3$	$\left(\frac{m_\mu^{\text{red}}}{m_\mu}\right)^3$
^{1}H	5.58569468	0.84075	1.67353283809945	0.998368814	0.726178616
^{2}H	0.85743823	2.12778	3.34449468647752	0.999183336	0.848431392
^{3}H	5.95792488	1.7591	3.34449468647752	0.999454538	0.895157605

Journal of Physics: Conference Series **3027** (2025) 012001 doi:10.1088/1742-6596/3027/1/012001

Table A2. Calculated hyperfine splittings for muonic (in meV) and normal hydrogen (in MHz) for different nuclear charge and magnetization models (for details see text) using the free lepton masses. Experimental data taken from [38] ($1s$ state of ^{1}H, ^{2}H, ^{3}H)), [39] (^{1}H $2s$), [40] (^{2}H $2s$), [41] (^{1}H $2p_{1/2}$), [42] (μ^1H $2s$) and [43] (μ^2H $2s$). For the nuclear parameters used to model the finite-size nuclei see appendix (Table A1). Multiplication with the respective factor $\left(\frac{m^{\text{red}}}{m}\right)^3$ from Table A1 yields estimates for reduced-mass corrected values.

atom	**state**	**exp** meV	**model with free mass m_μ** meV		
			point-like	**full sphere**	**spherical shell**
μ^1H	$1s$	—	251.299	249.934	249.653
μ^1H	$2s$	22.809	31.413	31.243	31.208
μ^2H	$1s$	—	57.864	57.072	56.909
μ^2H	$2s$	6.275	7.233	7.134	7.114
μ^3H	$1s$	—	268.048	265.008	264.385
μ^3H	$2s$	—	33.507	33.127	33.049
μ^1H	$2p_{1/2}$	—	10.471	10.471	10.471
μ^1H	$2p_{3/2,\pm1/2}$	—	2.094	2.094	2.094
μ^1H	$2p_{3/2,\pm3/2}$	—	6.282	6.282	6.282

atom	**state**	**exp** MHz	**model with free mass m_e** MHz		
			point-like	**full sphere**	**spherical shell**
^{1}H	$1s$	1420.406	1421.273	1421.236	1421.228
^{1}H	$2s$	177.557	177.665	177.660	177.659
^{2}H	$1s$	327.834	218.174	218.160	218.157
^{2}H	$2s$	40.925	27.273	27.271	27.270
^{3}H	$1s$	1516.701	1515.987	1515.903	1515.886
^{3}H	$2s$	—	189.505	189.494	189.492
^{1}H	$2p_{1/2}$	59.22	59.221	59.246	59.243
^{1}H	$2p_{3/2,\pm1/2}$	—	11.843	11.870	11.853
^{1}H	$2p_{3/2,\pm3/2}$	—	35.530	35.609	35.560